

## Forcing and Sampling of Ocean General Circulation Models: Impact of High-Frequency Motions\*

STEVEN R. JAYNE

*MIT-WHOI Joint Program in Oceanography, Woods Hole Oceanographic Institution, Woods Hole, Massachusetts*

ROBIN TOKMAKIAN

*Department of Oceanography, Naval Postgraduate School, Monterey, California*

17 September 1996 and 13 December 1996

### ABSTRACT

Significant inertial oscillations are present in all primitive equation ocean general circulation models when they are forced with high-frequency (period order of days) wind stress fields. At specific latitudes the energy of the wind stress forcing near the frequency of the inertial oscillations excites large amplitudes in the surface kinetic energy. The frequently used strategy of subsampling model output at several day intervals then leads to aliasing of the energetic inertial currents into lower frequencies that vary with latitude, which severely corrupts even integral quantities like meridional heat transport. This note discusses the effect of forcing and sampling at short periods. Schemes are provided that will remove the aliased energy from the model fields stored for later analysis.

### 1. Introduction

Inertial oscillations arise as simple solutions to the momentum equations for rotating fluid. In the ocean, these motions are known to be energetic, and it should therefore not be surprising that they are significant in numerical models of the ocean driven by realistic high-frequency forcing. Long time series of realistic wind stress fields are now available four times per day for forcing ocean general circulation models (OGCM) and therefore the effects of associated inertial oscillations present in the models on model diagnostics need to be addressed. Two problems arise with respect to inertial oscillations in OGCMs. First, the temporal approximation form of the wind stress forcing can excite zonal bands of large amplitude oscillations. For example, if wind fields are not changed smoothly in time but are updated every 3 days, the step function resonantly forces the inertial oscillations at specific latitudes. Second, most analyses of OGCM output for climate research or process studies are unconcerned about processes at timescales as short as the inertial period. However, if

the prognostic fields are output at any interval greater than one-half the inertial period, instantaneous sampling will alias inertial oscillations into lower frequencies that vary with latitude.

Recent analysis of high-resolution primitive equation models [Parallel Ocean Climate Model (POCM) with  $1/4^\circ$  resolution (Semtner and Chervin 1992; Stammer et al. 1996) and Los Alamos Parallel Ocean Project (POP11) with  $1/6^\circ$  resolution (Dukowicz and Smith 1994; Fu and Smith 1996)] as well as lower resolution OGCMs [e.g., the global MIT model with  $1^\circ$  resolution (Marshall et al. 1997a,b)] all show unrealistic features in the output velocity fields ( $u$  and  $v$ ) subsampled every 3 days and the associated diagnosed field of eddy kinetic energy (EKE) that result from the aliasing of inertial oscillations generated by the high-frequency wind stress forcing fields. To understand and to remove this unrealistic signal from future model runs, we have analyzed the sensitivity of the model inertial motions and the model output on the temporal forcing and the sampling period. Both aspects are addressed in this note. To do so, the temporal forcing was changed from uninterpolated step functions to a linear interpolant of the data. The sampling scheme is modified to filter out oscillations at frequencies higher than the Nyquist frequency prior to the model fields being output.

Tests are performed using the  $1/4^\circ$  resolution POCM. The version of the model is the same as described in Stammer et al. (1996). It is a primitive equation model on a Mercator grid (nominal resolution of  $1/4^\circ$ ) with 20

---

\*Woods Hole Oceanographic Institution Contribution Number 9355.

---

Corresponding author address: Steven Jayne, Woods Hole Oceanographic Institution, Clark 3, MS 21, Woods Hole, MA 02543-1541. E-mail: surje@sea.mit.edu

TABLE 1. Summary of test runs with varying forcing periods, functional forms, and sampling periods.

Test number	Wind forcing	Interpolation	Sampling
Original (PCOM_4B)	3 day	no	3-day snapshot
1	3 day	no	hourly
2	3 day	linear	hourly
3	1 day	linear	hourly

levels in the vertical. The model's surface momentum is forced with realistic wind stress fields derived from the twice-daily European Centre for Medium-Range Weather Forecasts (ECMWF) 10-m wind fields. The resulting wind stress fields are interpolated in space using bi-cubic spline fits onto the model grid. The changes of the present runs relative to the standard run discussed in Stammer et al. (1996) are related to 1) the temporal wind forcing and 2) the sampling of the prognostic variables, which are summarized in Table 1. All runs were initiated from the same point in time, 23 February 1993, defined by the date of the ECMWF wind stress fields and the initial prognostic 3D model fields from the run of POCM\_4B. Sampling of POCM\_4B was instantaneous snapshots of the model's prognostic variables (velocities, temperature, salinity, and sea surface elevation) every 3 days. The model time step is 1/2 h. In this study, the model's prognostic variables were also sampled hourly along several lines, meridional and zonal, to determine the differences resulting from how each run was being forced. For POCM\_4B and test 1, the wind stress fields were held constant over a 3-day period, whereas for tests 2 and 3 the wind stress fields were linearly interpolated to each time step. Section 2 focuses on the forcing problem and section 3 discusses the possible remedies to remove the aliasing in the sampled fields.

## 2. Changes in the forcing of the model

Inertial oscillations are a well-studied phenomenon in the ocean (Fu 1981; Gill 1982). A simple model of inertial oscillations can be found by a reduction of the momentum equations:

$$\begin{aligned} \frac{\partial u}{\partial t} - fv &= \tau_x(t) - ru \\ \frac{\partial v}{\partial t} + fu &= \tau_y(t) - rv, \end{aligned} \quad (1)$$

where  $u$  is the zonal component of velocity and  $v$  is the meridional component of velocity;  $f = 2\Omega \sin(\phi)$  is the Coriolis parameter in which  $\Omega$  is the angular rotation rate of the earth and  $\phi$  is the latitude;  $\tau_x$  and  $\tau_y$  are the zonal and meridional components of the wind stress, respectively; and  $r$  is the decay timescale for a linear dissipation. This coupled set of differential equations can be solved to give

$$u + iv = e^{-if't} e^{-rt} \int e^{if't} e^{rt} (\tau_x(t) + i\tau_y(t)) dt, \quad (2)$$

where  $i = \sqrt{-1}$ . This solution has a strong resonance at the frequency  $-f$ , limited only by the presence of dissipation, so any energy in the forcing at that frequency will excite significant amplitude inertial oscillations. In a statistical sense, the amplitude response of the inertial oscillations can be understood by knowing the characteristics of the rotary spectrum for the forcing function  $\tau(t)$ . The spectral response,  $S_{u+iv}(\omega)$ , of Eq. (2) is given by

$$S_{u+iv}(\omega) = \frac{S_\tau(\omega)}{(\omega + f - ir)^2}, \quad (3)$$

where  $\omega$  is the angular frequency and  $S_\tau(\omega)$  is the power spectrum of the wind forcing (Priestley 1981).

In the real world, the wind stress varies on all time-scales and  $S_\tau(\omega)$  is a continuous function. However, the available high-frequency wind stress datasets are provided at best only four times a day as compared to model time steps of about an hour. What is the most appropriate method to interpolate the provided wind fields to the model time steps in such a way to best preserve the real high-frequency wind stress spectrum? Three methods are possible: 1) a wind stress field kept constant over an observation period (series of step function), 2) a wind field linearly interpolated between observation time points, and 3) a cubic spline interpolation (or other higher order method, such as Hermite interpolation) of the wind forcing. At frequencies lower than the Nyquist frequency of the wind stress data, the power spectrum of the forcing is determined by the data. However, at frequencies higher than the Nyquist frequency of the data, the power spectrum is dominated by the autocorrelation behavior of the functional form used for the interpolation. If the available data has a Nyquist period that is of order days, then the inertial frequency for latitudes away from the equator will lie in the portion of the power spectrum that is determined by the interpolation and, accordingly, the forcing of inertial oscillations will be a function of the interpolation scheme. If one is not interested in inertial motions, the interpolation method therefore should be chosen carefully such that its high-frequency characteristics are smooth and continuous to avoid artificial high-frequency motions. However, there may be issues related to mixed layer physics parameterizations where the inertial energy is needed (Large et al. 1994).

Since most high-frequency wind stress datasets will require some form of interpolation to be used as forcing in an OGCM, it is necessary to discuss the implications of various methods. The two methods discussed here are 1) keeping the wind stress constant over a data period since it is relevant to the available POCM output and 2) the more commonly used linear interpolation. In order to establish a notational framework, we first de-

note a sequence of indices for the forcing functions, where  $i = 0, 1, 2, 3, \dots$  are the times when we have data available and  $j = 0, 1, 2, 3, \dots$  are the model time steps that we are interpolating the original data to. If the model wind stress is simply updated once per 3 days without any interpolation, the forcing function is written

$$\tau_i^j = a_i \quad (4)$$

for all  $j = 0, 1, 2, \dots$ , where  $a_i$  is simply the wind stress read in from the data files. If we make the assumption that the  $a_i$  are uncorrelated, then the power spectrum of the wind forcing at frequencies higher than the Nyquist frequency of the data can be found analytically by taking the Fourier transform of the autocorrelation of the interpolant (Bracewell 1986). For the case of the series of step functions, the power spectrum is given by

$$S_\tau(\omega) \propto \frac{1 - \cos(\omega h)}{(\omega h)^2}, \quad (5)$$

where  $h = 3$  days. The more advanced technique of linearly interpolating to each time step between the available data is denoted by

$$\tau_i^j = a_i + b_i(j\Delta t), \quad (6)$$

where  $b_i = (a_{i+1} - a_i)/h$ , where  $a_i$  is again the wind stress read in from the data files for that day, and  $a_{i+1}$  is the wind stress for the 3 days later,  $\Delta t = 1/2$  h and again  $h = 3$  days. This form of the forcing has the power spectrum

$$S_\tau(\omega) \propto \frac{3 - 4\cos(\omega h) + \cos(2\omega h)}{(\omega h)^4}. \quad (7)$$

It can be seen that both of these methods have zeros in the power spectrum at  $\omega h = 2\pi, 4\pi, 6\pi, \dots$ , which, still assuming that  $h = 3$  days, correspond to periods of 3 days, 1.5 days, 1 day, etc. Any motions at these periods will be only weakly forced compared with motions with frequencies at  $\omega h \approx 3\pi, 5\pi, 7\pi, \dots$  (periods of 2 days, 1.2 days, 0.86 days, etc.), which are located at local maxima of both the forcing functions spectra. If the zeros correspond to the period of the inertial oscillations at a given latitude, there will be a marked depletion in the amplitude of the inertial oscillations at that latitude since there is much less energy in the forcing to drive them. Whereas if the inertial period is at a local maximum in the power spectrum of the forcing function, the inertial oscillations will be forced much more strongly. Additionally, between the zeros in the power spectrum, the peaks fall off at a rate of  $\omega^{-2}$  for the uninterpolated forcing and  $\omega^{-4}$  for the linearly interpolated forcing. This should result in a noticeable depletion in the strength of the inertial oscillations at latitudes where their frequency is higher than the Nyquist frequency of the data and a more general weakening in the high-frequency energy in the model overall.

These effects can be seen in two different ways in the hourly sampled model data. First, we can consider

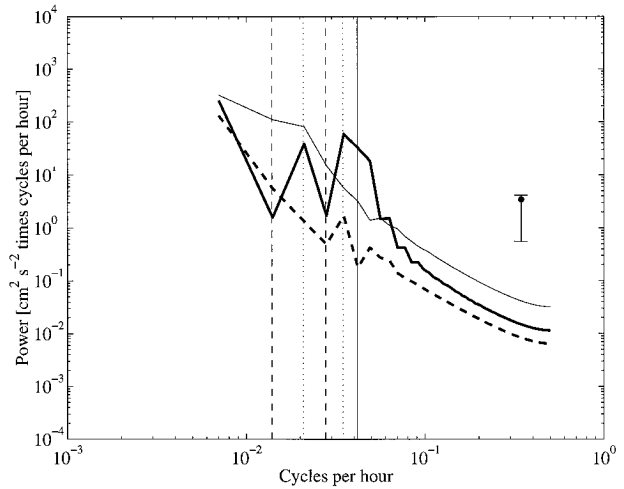


FIG. 1. Frequency spectra of the  $u$  component of velocity at  $30^\circ\text{N}$ ,  $200^\circ\text{E}$  in the North Pacific for tests 1 with once per 3 days uninterpolated forcing (thin solid line), test 2 with once per 3 days linearly interpolated forcing (dashed line), and test 3 with once per day linearly interpolated forcing (heavy solid line). Vertical dashed lines are at the expected minima (3 days and 1.5 days) and dotted lines are the expected maxima (2 days and 1.2 days). The thin solid vertical line is at the inertial frequency.

the power spectrum of the velocity at a single point in the ocean as a function of frequency. If the velocities in the surface layer are strongly coupled to the forcing function at high frequencies, it is expected that the shape of the spectrum for the velocities will be strongly influenced by the shape of the forcing spectrum. Figure 1 shows the power spectrum of the  $u$  component of velocity sampled every hour for the surface layer at  $30^\circ\text{N}$ ,  $200^\circ\text{E}$  for the three different forcing tests. Most noticeable is the deficit of energy at frequencies corresponding to 3 days and 1.5 days and peaks of energy at 2 days and 1.2 days when the forcing function is derived from the once per 3 day data in both the uninterpolated and linearly interpolation methods. The comparison at higher frequencies becomes more difficult due to noisiness of the spectrum and to the strong spectral peak from the inertial oscillations. At  $30^\circ\text{N}$  the peak in the spectrum due to the inertial oscillations corresponds to approximately 1 day, where a spectral gap from the forcing is expected. But, the energy in the higher frequencies do indeed show an overall weakening of almost an order of magnitude when the linear interpolant is used. This is consistent with the analytic forms derived above. When the wind stress forcing is derived from daily data instead of data every 3 days, the spectrum fills out at periods longer than 2 days, but now shows a depletion at the 1-day period, again consistent with the previous arguments if  $h = 1$  day.

The second way to compare these analytic arguments to the model results is to consider the amplitude of the inertial oscillations as a function of latitude. Since the frequency of the inertial oscillations increases with increasing latitude, the inertial oscillations will be forced

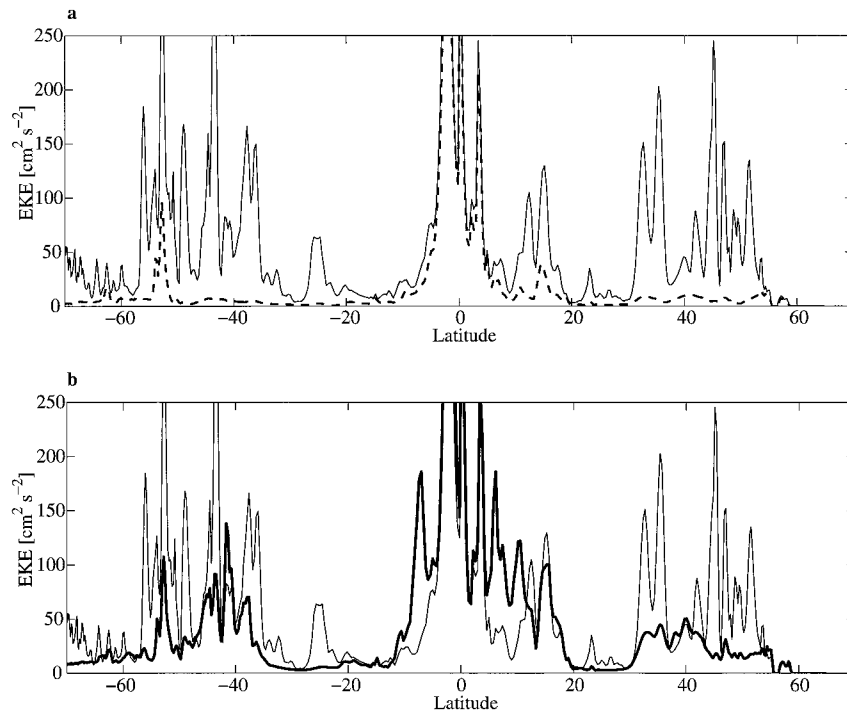


FIG. 2. EKE along 200°E for forcing with once per 3 days uninterpolated wind stress (thin solid line) and with (a) once per 3 days linearly interpolated forcing (dashed line) and (b) once per day linearly interpolated forcing (heavy solid line). EKE is in  $\text{cm}^2 \text{s}^{-2}$ .

by varying energy according to Eq. (5) and (7), and therefore we expect to see minima in the amplitude of the inertial oscillations where  $S_r(\omega)$  is small and maxima where it is large. At most latitudes the inertial oscillations dominate the EKE in the hourly sampled data, so we use the EKE as a proxy for the strength of inertial oscillations. Figure 2 shows the EKE as a function of latitude for the three tests. Figure 2a compares the uninterpolated forcing (test 1) with the linearly interpolated forcing (test 2). The EKE from test 1 shows bands of sharp peaks alternating with bands of low energy. The bands of low energy correspond directly to latitudes where the forcing spectra have minima, namely, where  $\omega h = fh = 2\pi, 4\pi, 6\pi, \dots$  corresponding to

$$\phi = \text{asin}\left(\frac{2n\pi}{2\Omega h}\right) \quad \text{for } n = 1, 2, 3, \dots, \quad (8)$$

which for once per 3 day data ( $h = 3 \text{ days}$ ) occur at the latitudes  $9.6^\circ, 19.4^\circ, 29.9^\circ, 41.7^\circ,$  and  $56.2^\circ$ . The most noticeable effect from the change to linear interpolation is the significant decrease in strength of the EKE away from the equator when the linear interpolation is used. This is driven by the faster decay of wind stress energy at high frequencies using the linear interpolation method instead of the uninterpolated method. The change to using daily wind stress values with linear interpolation (Fig. 2b) increases the energy at most latitudes, but a minimum still occurs at latitude  $29.9^\circ$  where  $fh = 2\pi$  for  $h = 1 \text{ day}$ . Better methods would be either

real forcing fields every time step or a spline fit applied to the original data to interpolate to each time step. Both of these solutions, however, are logistically difficult to implement. This leads directly to the next section on how to remedy the problems shown.

### 3. Solutions to aliasing of the inertial frequencies

In POCM, prognostic fields are output every 3 model days, whereas the inertial period varies with latitude from  $1/2$  a day at the poles to infinitely long at the equator. Therefore, the saved model record only resolves the inertial oscillations where their period is greater than 6 days corresponding to within about  $5^\circ$  of the equator. At higher latitudes where the sampling does not resolve the inertial oscillations, they are aliased in time so that they impersonate oscillations with much longer periods. The aliasing frequencies follow from

$$\omega = f - \frac{2n\pi}{\Delta t} \quad (9)$$

with  $\Delta t = 3 \text{ day}$  sampling period, and  $n = 0, 1, 2, 3, \dots$  such that  $|\omega| \leq \pi/\Delta t$ . Because  $f$  varies meridionally, the aliased frequency is also a function of latitude. Shown in Fig. 3 is the true period of inertial oscillations and their aliased period as a function of latitude for sampling periods ( $\Delta t$ ) of once per day and once per 3 days. The latitudes at which the aliased period of the inertial motions go to infinity (the frequency,  $\omega = 0$ )

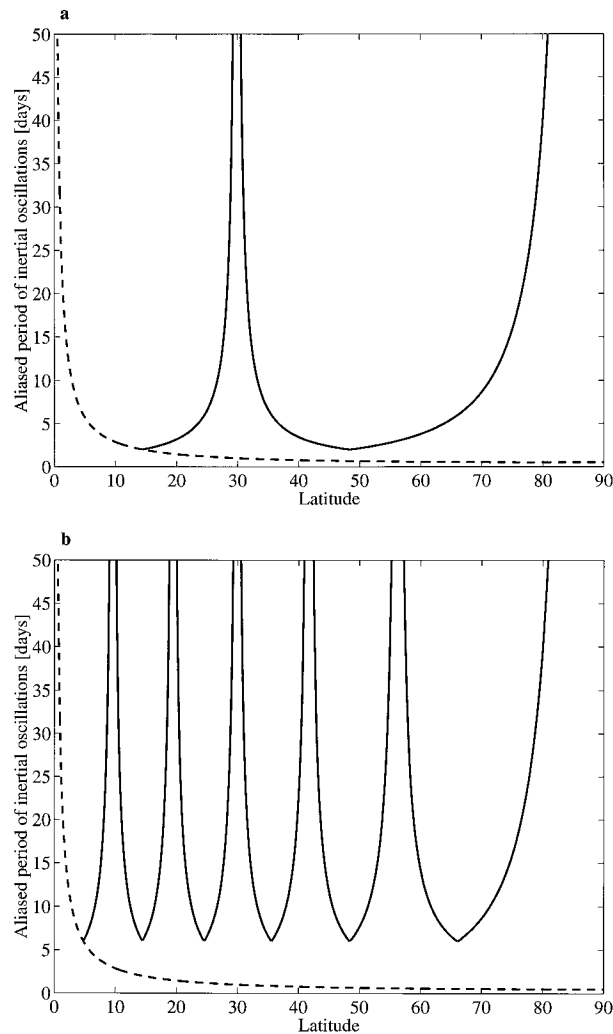


FIG. 3. The true period of inertial oscillations (dashed) and their aliased period (solid) as a function latitude for sampling at (a) once per day and (b) once per 3 days.

follow from (8), substituting  $\Delta t$  for  $h$  and are at  $9.6^\circ$ ,  $19.4^\circ$ ,  $29.9^\circ$ ,  $41.7^\circ$ , and  $56.2^\circ$ . At these latitudes, the inertial oscillations are aliased into the time mean. In between these latitudes there are broad bands where the period of the inertial oscillations is aliased to a period longer than the Nyquist frequency of the output data.

It is impossible to eliminate aliasing due to subsampling of the model; however, one can reduce the amplitude of the aliased inertial oscillation signal in the true EKE by saving filtered estimates of the prognostic variables instead of using instantaneous dumps of the variables every 3 days. An ideal filtering scheme would remove from the output all oscillations at frequencies higher than the Nyquist frequency of the output data. However, such filtering schemes would require knowledge of the entire time history of the model to make a filtered estimate at any given time point, which is not realistic in an OGCM due to memory and/or disk storage

requirements. But filters can be applied to the model during the run, which only require knowledge from single time steps over the output period. There is an extensive literature on the design and use of filters (Priestly 1981). Among the host of possible choices, the running average (or boxcar filter) and Hamming filter are commonly used and easy to implement. Note that a low-pass filter ( $> 9$  days) applied to the POCM4B output will remove much of the spurious eddy energy associated with the inertial motions, but not where it was aliased into the mean fields.

#### a. Average fields

The running average requires only summing the variables in time over a given period and dividing by the number of time points included in the sum. If the period is chosen to be significantly greater than the period of the inertial oscillations, inertial energy will be removed from the output. A comparison of the zonally averaged EKE as a function of latitude for the original run with the result of tests 2 and 3 averaged over 3-day periods is shown in Fig. 4. The dominant feature to recognize is the removal of the large peaks in the EKE associated with the inclusion of the inertial oscillations in lower-frequency time-dependent motions. In the thin bands of low EKE in the unfiltered estimate near  $9.6^\circ$ ,  $19.4^\circ$ ,  $29.9^\circ$ ,  $41.7^\circ$ , and  $56.2^\circ$ , the inertial oscillations do not contribute to the EKE since their aliased period is very long. Whereas in the filtered estimate, the inertial oscillations are removed from the output before the EKE calculation. Therefore, at these latitudes there is very little difference between the filtered and unfiltered estimates of EKE. The minor differences between tests 2 and 3 are real effects of the higher-frequency forcing used in test 3.

#### b. Hamming filter

The boxcar filter is the simplest filter to implement, requiring only that the model save the mean of the prognostic variables every three days. However, unless the length of the boxcar filter is much greater than the period of the oscillations to be removed or there are an integer number of complete oscillations within the period of the filtering, the boxcar filter can only weakly damp their amplitude due to the significant sidelobes in the frequency domain of the boxcar filter. It is well known that tapering the sides of the filter in the time domain reduces the amplitude of the sidelobes in the frequency domain. An excellent candidate for this application is the Hamming filter since it minimizes the sidelobes in the frequency domain (Priestly 1981). The Hamming filter would be implemented in a similar fashion as the boxcar filter; however, a weighting coefficient used for each time step is changed at each time step. The coefficients are given by the formula

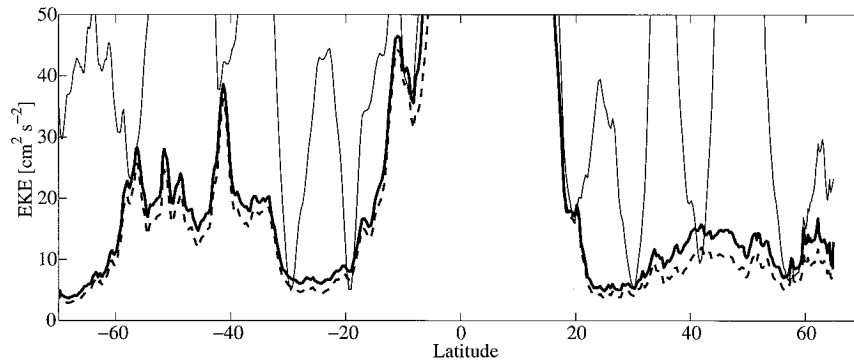


FIG. 4. Zonal average EKE for April 1993 for the original run, which used once per 3 day uninterpolated forcing and once per 3 day instantaneous sampling (thin solid line), test 2 with once per 3 day linearly interpolated forcing and 3-day averaged samples (dashed line), and test 3 with once per day linearly interpolated forcing and 3-day averaged samples (heavy solid line). EKE is in  $\text{cm}^2 \text{s}^{-2}$ .

$$w(k) = 0.54 - 0.46 \cos\left(\frac{2\pi k}{n-1}\right),$$

$$0 \leq k \leq n-1, \quad (10)$$

where  $n$  is the number of time steps in 3 days. We can compare the effectiveness of the boxcar and Hamming filters at damping an oscillation at the inertial frequency as a function of latitude. Figure 5 shows the damping coefficient of the filtered inertial oscillation as a function of latitude for the boxcar and Hamming filters. For a sampling period of 3 days, the filtered inertial energy poleward of  $\pm 19^\circ$  is less than 1% of its original magnitude, whereas over a similar range, the boxcar filter is about an order of magnitude less effective.

The inertial oscillations present in the model not only affect the velocity fields and eddy kinetic energy, but also higher-order products. The meridional heat transport is very sensitive to the aliasing induced by the

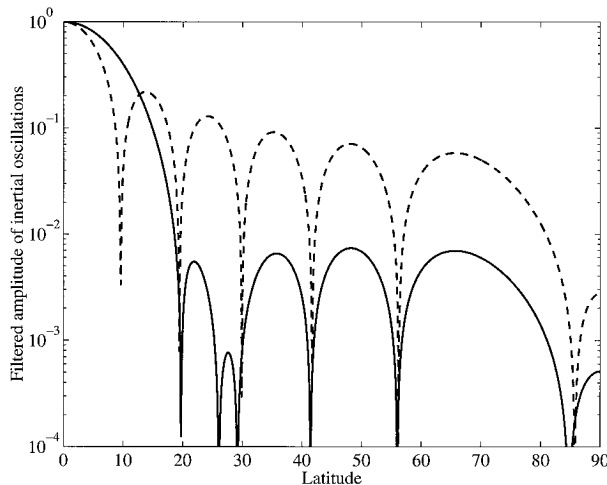


FIG. 5. Damping response coefficient for inertial oscillations as a function of latitude for a Hamming filter (solid line) and a boxcar filter (dashed line).

inertial oscillations because in the model they carry a large amount of heat in the surface layer. It has a very large amplitude oscillation at the inertial frequency, as can be seen in Fig. 6a. The heat transport across  $25^\circ\text{N}$  in the Atlantic Ocean calculated from hourly output from test case 1 shows an oscillation at the inertial frequency with an amplitude of about 1 petawatt. Overlaying an arbitrary 3-day subsampling on it clearly gives a much different picture than the full time series shown from hourly sampling. In Fig. 6b, the response in the zonal heat transport at  $25^\circ\text{N}$  with the boxcar filter is compared to same using a Hamming filter with a width of 3 days. The Hamming filter (solid line) damps out the inertial oscillations much more effectively than the boxcar filter (dashed line). From these considerations, it appears that the Hamming filter is the most appropriate to use to remove the inertial oscillations from the model records.

#### 4. Conclusions

This note has discussed the various implications of using high-frequency forcing and associated sampling resulting in the sampled prognostic fields containing aliased signals due to inertial oscillations. It has been shown that inertial motions are aliased into longer period motions whose frequency depends on the latitude and sampling rate. At some latitude and subsampling period combinations, the inertial motions can be aliased into the mean fields. The method used to perform the temporal interpolation of the wind stress fields can cause the high-frequency power spectrum to be distorted. For an investigator wishing to study high-frequency motions, such as inertial oscillations, these arguments relate that it would be best to examine the model state at a very high frequency and force the model with high-frequency fields. However, for an investigator studying the general circulation of the ocean, we recommend that some type of filtering prior to saving fields for later analysis be incorporated in the model run to remove the

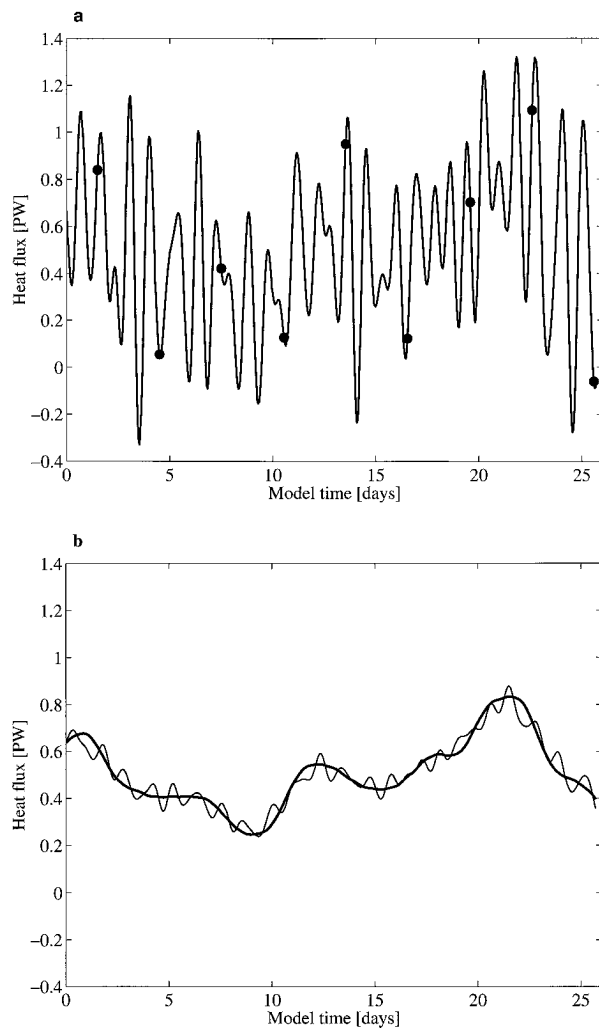


FIG. 6. (a) Unfiltered heat transport time series at 25°N in the Atlantic with the dots representing arbitrary once per 3 day sampling. (b) Same results but using a 3-day running boxcar filter (thin solid line) and a 3-day running Hamming filter (heavy solid line) on the heat transport data.

inertial oscillations. We also suggest that even when new forcing fields are read in every day, they need to be interpolated to every time step to remove steps in the forcing of the model.

*Acknowledgments.* Funding for this research came

from the Department of Energy's Office of Health and Environmental Research under CHAMP (Computer Hardware, Advanced Mathematics, Model Physics) and the National Science Foundation's Physical Oceanography Program under WOCE (RT) and the Department of Defense under a National Defense Science and Engineering Graduate Fellowship (SRJ). The National Center for Atmospheric Research provided the computational resources for simulations. Jochem Marotzke, Bert Semtner, Detlef Stammer, and Carl Wunsch nudged us to look for solutions to this problem of aliasing in sampling and forcing of high-frequency motions in numerical models. We thank Mike Spall and two anonymous reviewers for their helpful comments and suggestions. Financial support was also contributed by the Tokyo Electric Power Company through the TEPCO/MIT Environmental Research Program.

#### REFERENCES

- Bracewell, R. N., 1986: *The Fourier Transform and Its Applications*. McGraw-Hill, 444 pp.
- Dukowicz, J., and R. D. Smith, 1994: Implicit free-surface method for the Bryan-Cox-Semtner ocean model. *J. Geophys. Res.*, **99**, 7991-8014.
- Fu, L.-L., 1981: Observations and models of inertial waves in the deep ocean. *Rev. Geophys. Space Phys.*, **19**, 141-170.
- , and R. D. Smith, 1996: Global ocean circulation from satellite altimetry and high-resolution computer simulation. *Bull. Amer. Meteor. Soc.*, **77**, 2625-2636.
- Gill, A. E., 1982: *Atmosphere-Ocean Dynamics*. Academic Press, 662 pp.
- Large, W. G., J. C. McWilliams, and S. C. Doney, 1994: Oceanic vertical mixing: A review and a model with nonlocal boundary layer parameterization. *Rev. Geophys.*, **32**, 363-403.
- Marshall, J., C. Hill, L. Perelman, and A. Adcroft, 1997a: Hydrostatic, quasi-hydrostatic and non-hydrostatic ocean modeling. *J. Geophys. Res.*, **102**, 5733-5752.
- , A. Adcroft, C. Hill, L. Perelman, and C. Heisey, 1997b: A finite-volume, incompressible Navier-Stokes model for studies of the ocean on parallel computers. *J. Geophys. Res.*, **102**, 5753-5766.
- Priestley, M. B., 1981: *Spectral Analysis and Time Series*. Vol. 1: *Univariate Series*; Vol. 2: *Multivariate Series, Prediction and Control*. Academic Press, 890 pp plus appendices (combined edition).
- Semtner, A. J., and R. M. Chervin, 1992: Ocean general circulation from a global eddy-resolving model. *J. Geophys. Res.*, **97**, 5493-5550.
- Stammer, D., R. Tokmakian, A. J. Semtner, and C. Wunsch, 1996: How well does a 1/4° global circulation model simulate large-scale oceanic observations? *J. Geophys. Res.*, **101**, 25 779-25 811.